

# PAC-BAYESIAN META-LEARNING WITH IMPLICIT PRIOR

**Cuong C. Nguyen**

School of Computer Science  
The University of Adelaide  
Adelaide, SA 5005, Australia  
cuong.nguyen@adelaide.edu.au

**Thanh-Toan Do**

Department of Computer Science  
University of Liverpool  
Liverpool, UK  
thanh-toan.do@liverpool.ac.uk

**Gustavo Carneiro**

School of Computer Science  
The University of Adelaide  
Adelaide, SA 5005, Australia  
gustavo.carneiro@adelaide.edu.au

## ABSTRACT

We introduce a new and rigorously-formulated PAC-Bayes few-shot meta-learning algorithm that implicitly learns a prior distribution of the model of interest. Our proposed method extends the PAC-Bayes framework from a single task setting to the few-shot learning setting to upper-bound generalisation errors on unseen tasks and samples. We also propose a generative-based approach to model the shared prior and the posterior of task-specific model parameters more expressively compared to the usual diagonal Gaussian assumption. We show that the models trained with our proposed meta-learning algorithm are well calibrated and accurate, with state-of-the-art calibration and classification results on few-shot classification (mini-ImageNet and tiered-ImageNet) and regression (multi-modal task-distribution regression) benchmarks.

## 1 INTRODUCTION

One unique ability of humans is to be able to quickly learn new tasks with only a few *training* examples. This is due to the fact that humans tend to exploit prior experience to facilitate the learning of new tasks. Such exploitation is markedly different from conventional machine learning approaches, where no prior knowledge (e.g. training from scratch with random initialisation) (Glorot & Bengio, 2010), or weak prior knowledge (e.g., fine tuning from pre-trained models) (Rosenstein et al., 2005) are employed to learn a new task. This motivates the development of novel learning algorithms that can effectively encode the knowledge learnt from training tasks, and exploit that knowledge to quickly adapt to future tasks (Lake et al., 2015).

Prior knowledge can be helpful for future learning only if all tasks are assumed to be distributed according to a latent task distribution. Learning this latent distribution is, therefore, useful for solving an unseen task, even if the task contains a limited number of training examples. Many approaches have been proposed and developed to achieve this goal, namely: *multi-task learning* (Caruana, 1997), *domain adaptation* (Bridle & Cox, 1991; Ben-David et al., 2010) and *meta-learning* (Schmidhuber, 1987; Thrun & Pratt, 1998). Among these, meta-learning has flourished as one of the most effective methods due to its ability to leverage the knowledge learnt from many training tasks to quickly adapt to unseen tasks.

Recent advances in meta-learning have produced state-of-the-art results in many benchmarks of few-shot learning data sets (Santoro et al., 2016; Ravi & Larochelle, 2017; Munkhdalai & Yu, 2017; Snell et al., 2017; Finn et al., 2017; Zhang et al., 2018; Rusu et al., 2019). Learning from a few training examples is often difficult and easily leads to over-fitting, especially when no model uncertainty is taken into account. This issue has been addressed by several recent probabilistic meta-learning approaches that incorporate model uncertainty into prediction, notably LLAMA that is based on

Laplace method (Grant et al., 2018), or PLATIPUS (Finn et al., 2017), Amortised Bayesian Meta-learner (ABML) (Ravi & Beatson, 2019) and VERSA (Gordon et al., 2019) that use variational inference (VI). However, these works have not thoroughly investigated the generalisation errors for unseen tasks and unseen samples, resulting in limited theoretical generalisation guarantees. Moreover, most of these papers are based on variational functions that may not represent well the richness of the underlying distributions. For instance, a common choice for the variational function relies on the diagonal Gaussian distribution, which can potentially worsen the prediction accuracy given its limited representability.

In this paper, we address the two problems listed above with the following technical novelties: (i) derivation of a rigorous upper-bound for the generalisation errors on unseen tasks and samples of few-shot learning setting based on PAC-Bayes framework, and (ii) proposal of a novel implicit modelling approach to expressively represent the learning of unseen tasks. Our evaluation shows that the models trained with our proposed meta-learning algorithm is at the same time well calibrated and accurate, with state-of-the-art results in few-shot classification (mini-ImageNet and tiered-ImageNet) and regression (multi-modal task-distribution regression) benchmarks in terms of accuracy, Expected Calibration Error (ECE) and Maximum Calibration Error (MCE).

## 2 RELATED WORK

Our paper is related to Bayesian few-shot meta-learning techniques that have been developed to incorporate uncertainty into model estimation. LLAMA (Grant et al., 2018) employs the Laplace method to extend the deterministic estimation assumed in MAML to a Gaussian distribution. However, the need to estimate and invert the Hessian matrix makes this approach computationally challenging for large-scale models, such as deep neural networks. Variational inference (VI) addresses such scalability issue – remarkable examples of VI-based methods are PLATIPUS (Finn et al., 2018), BMAML (Yoon et al., 2018), ABML (Ravi & Beatson, 2019) and VERSA (Gordon et al., 2019). Although these VI-based approaches have demonstrated impressive results in regression, classification as well as reinforcement learning, they do not provide any theoretical guarantee on generalisation errors for unseen tasks and unseen samples within a task. Moreover, the overly-simplified family of diagonal Gaussian distributions that model task-specific model parameters used in most of these works limits the expressiveness of the variational approximation, resulting in a less accurate prediction.

Our work is also related to the PAC-Bayes framework used in meta-learning that upper-bounds generalisation errors with certain confidence levels (Pentina & Lampert, 2014; Amit & Meir, 2018). These previous works follow non-Bayesian approaches to learn the shared prior<sup>1</sup> and task-specific model parameters simultaneously. These approaches are, therefore, applicable for multi-task learning setting (Amit & Meir, 2018, Section 4.4), in which the learning is carried out on a small number of tasks where each task consists of thousands of training examples. In contrast, our proposed approach is based on a variant of the empirical Bayesian method, where the learning is cast into a bi-level optimisation (Bard, 2013; Von Stackelberg, 2010). In the lower-level, the shared prior and task-specific model parameters are correlated explicitly through a variational Bayes inference, while in the upper-level, the shared prior is learnt by minimising the PAC-Bayes bound using the correlation learnt in the lower-level. Therefore, our proposed method is suitable for few-shot learning, in which the learning is performed on millions of training tasks where each task consists of a few training examples.

## 3 METHODOLOGY

### 3.1 FEW-SHOT META-LEARNING

We use the notation of *task environment* (Baxter, 2000) to describe the unknown distribution  $p(\mathcal{T})$  over a family of tasks. Each task  $\mathcal{T}_i$  sampled from  $p(\mathcal{T})$  is indexed by  $i \in \{1, \dots, T\}$  and associated with a dataset  $\mathcal{D}_i$  consisting of two disjoint data subsets: an observable support set

<sup>1</sup>The usage of *posterior* in this paper does not always follow the Bayesian connotation, but depends on the context. In PAC-Bayes, the posterior and prior does not need to be correlated through the likelihood function as in standard Bayesian inference.

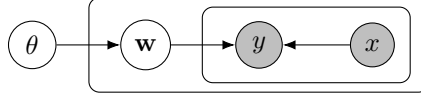


Figure 1: Hierarchical model used in few-shot, where  $\mathbf{w}$  is the task-specific model parameter, and  $\theta$  is the prior of  $\mathbf{w}$  shared across all tasks.

$\mathcal{D}_i^{(t)} = \{(\mathbf{x}_{ij}^{(t)}, y_{ij}^{(t)})\}_{j=1}^{m_i^{(t)}}$  ( $\mathbf{x} \in \mathbb{R}^d$  is an observable input and  $y \in \mathcal{Y}$  represents a label) and a hidden query set  $\mathcal{D}_i^{(v)}$ . Theoretically,  $\mathcal{D}_i^{(v)}$  has infinite examples, but during training, we are given a finite number of examples  $\hat{\mathcal{D}}_i^{(v)} = \{(\mathbf{x}_{ij}^{(v)}, y_{ij}^{(v)})\}_{j=1}^{m_i^{(v)}} \subset \mathcal{D}_i^{(v)}$ . The aim of few-shot learning is to accurately predict the output  $y_{ij}^{(v)}$  of any query input  $\mathbf{x}_{ij}^{(v)}$  sampled from the query set  $\mathcal{D}_i^{(v)}$ , when being given a small support set  $\mathcal{D}_i^{(t)}$ . We rely on a hierarchical model shown in Figure 1, where  $\mathbf{w}_i$  represents the model parameter for task  $\mathcal{T}_i$ , and  $\theta$  denotes the meta-parameter shared across all tasks (Grant et al., 2018).

We derive the objective function for the learning by applying Jensen’s inequality to lower-bound the log-evidence:

$$\begin{aligned} & \mathbb{E}_{\mathcal{D}_i \sim p(\mathcal{T})} \mathbb{E}_{(\mathbf{x}_{ij}^{(v)}, y_{ij}^{(v)}) \sim \mathcal{D}_i^{(v)}} \left[ \ln p(y_{i,1:m_i^{(t)}}^{(t)}, y_{ij}^{(v)} | \mathbf{x}_{i,1:m_i^{(t)}}^{(t)}, \mathbf{x}_{ij}^{(v)}) \right] \\ &= \mathbb{E}_{\mathcal{D}_i \sim p(\mathcal{T})} \mathbb{E}_{(\mathbf{x}_{ij}^{(v)}, y_{ij}^{(v)}) \sim \mathcal{D}_i^{(v)}} \left[ \ln \int p(y_{i,1:m_i^{(t)}}^{(t)}, y_{ij}^{(v)} | \mathbf{x}_{i,1:m_i^{(t)}}^{(t)}, \mathbf{x}_{ij}^{(v)}, \theta) p(\theta) d\theta \right] \\ &\geq \mathbb{E}_{\mathcal{D}_i \sim p(\mathcal{T})} \mathbb{E}_{(\mathbf{x}_{ij}^{(v)}, y_{ij}^{(v)}) \sim \mathcal{D}_i^{(v)}} \mathbb{E}_{q(\theta; \psi)} \left[ \ln p(y_{i,1:m_i^{(t)}}^{(t)}, y_{ij}^{(v)} | \mathbf{x}_{i,1:m_i^{(t)}}^{(t)}, \mathbf{x}_{ij}^{(v)}, \theta) \right] \\ &\quad - D_{\text{KL}} [q(\theta; \psi) \| p(\theta)], \end{aligned} \quad (1)$$

where  $q(\theta; \psi) > 0$ , parameterised by  $\psi$ , is a variational distribution for the meta-parameter  $\theta$ . In practice,  $q(\theta; \psi)$  is often assumed to be a Gaussian distribution.

The log-likelihood of the first term in (1) can be expanded following the hierarchical model shown in Figure 1, and lower-bounded by Jensen’s inequality:

$$\begin{aligned} & \ln p(y_{i,1:m_i^{(t)}}^{(t)}, y_{ij}^{(v)} | \mathbf{x}_{i,1:m_i^{(t)}}^{(t)}, \mathbf{x}_{ij}^{(v)}, \theta) \\ &= \ln \int p(y_{i,1:m_i^{(t)}}^{(t)}, y_{ij}^{(v)} | \mathbf{x}_{i,1:m_i^{(t)}}^{(t)}, \mathbf{x}_{ij}^{(v)}, \mathbf{w}_i) p(\mathbf{w}_i | \theta) d\mathbf{w}_i \geq -\mathcal{L}_{ij}^{(v)} - \mathcal{L}_i^{(t)}, \end{aligned} \quad (2)$$

where:

$$\mathcal{L}_{ij}^{(v)} = \mathbb{E}_{q(\mathbf{w}_i; \lambda_i)} \left[ -\ln p(y_{ij}^{(v)} | \mathbf{x}_{ij}^{(v)}, \mathbf{w}_i) \right], \quad (3)$$

$$\mathcal{L}_i^{(t)} = D_{\text{KL}} [q(\mathbf{w}_i; \lambda_i) \| p(\mathbf{w}_i; \theta)] - \sum_{k=1}^{m_i^{(t)}} \mathbb{E}_{q(\mathbf{w}_i; \lambda_i)} \left[ \ln p(y_{ik}^{(t)} | \mathbf{x}_{ik}^{(t)}, \mathbf{w}_i) \right], \quad (4)$$

and  $q(\mathbf{w}_i; \lambda_i) > 0$  is a variational distribution for  $p(\mathbf{w}_i | \mathbf{x}_{i,1:m_i^{(t)}}^{(t)}, y_{i,1:m_i^{(t)}}^{(t)}, \theta)$ .

Given (1) and (2), our objective function is to find the variation parameter  $\psi$  for  $q(\theta; \psi)$  to maximise the lower-bound, or, equivalently minimise the negation of the lower-bound:

$$\min_{\psi} \mathbb{E}_{\mathcal{D}_i \sim p(\mathcal{T})} \mathbb{E}_{(\mathbf{x}_{ij}^{(v)}, y_{ij}^{(v)}) \sim \mathcal{D}_i^{(v)}} \mathbb{E}_{q(\theta; \psi)} \left[ \mathcal{L}_{ij}^{(v)} + \mathcal{L}_i^{(t)} \right] + D_{\text{KL}} [q(\theta; \psi) \| p(\theta)]. \quad (5)$$

To evaluate the cost function in (5), we need to estimate the variational posterior  $q(\mathbf{w}_i; \lambda_i)$  of the task-specific model parameter  $\mathbf{w}_i$  in Jensen’s inequality of (2). The purpose of  $q(\mathbf{w}_i; \lambda_i)$  is to approximate the true posterior of  $\mathbf{w}_i$  given its prior  $\theta$  and observable data  $\mathcal{D}_i^{(t)}$ , which is  $p(\mathbf{w}_i | \mathcal{D}_i^{(t)}, \theta)$ . In Bayesian learning,  $p(\mathbf{w}_i | \mathcal{D}_i^{(t)}, \theta)$  is obtained through Bayes’ rule, and is often intractable, especially when the model used is a deep neural network. Hence, in practice, we use  $q(\mathbf{w}_i; \lambda_i)$  to

approximate  $p(\mathbf{w}_i | \mathcal{D}_i^{(t)}, \theta)$ . One way to obtain  $q(\mathbf{w}_i; \lambda_i)$  is to use VI, which minimises the KL divergence between the two distribution:

$$\begin{aligned} \lambda_i^* &= \arg \min_{\lambda_i} D_{\text{KL}} \left[ q(\mathbf{w}_i; \lambda_i) \parallel p(\mathbf{w}_i | \mathbf{x}_{i,1:m_i^{(t)}}^{(t)}, y_{i,1:m_i^{(t)}}^{(t)}, \theta) \right] \\ &= \arg \min_{\lambda_i} \mathcal{L}_i^{(t)} + \sum_{k=1}^{m_i^{(t)}} \underbrace{\ln p(y_{ik}^{(t)} | \mathbf{x}_{ik}^{(t)}, \theta)}_{\text{const. wrt } \lambda_i}, \end{aligned} \quad (6)$$

where  $\mathcal{L}_i^{(t)}$  is defined in Eq. 4.

The resulting cost function (excluding the constant term),  $\mathcal{L}_i^{(t)}$ , is often known as the variational free energy (VFE). Exactly minimising VFE in (6) is computationally challenging, so gradient descent is used with  $\theta$  as the initialisation:

$$\lambda_i \leftarrow \theta - \alpha_t \nabla_{\lambda_i} \mathcal{L}_i^{(t)}, \quad (7)$$

where  $\alpha_t$  is the learning rate and the truncated gradient descent consists of a single step (the extension to a larger number of steps is trivial).

Given  $q(\mathbf{w}_i; \lambda_i)$  obtained in (6), the objective function in (5) can be considered as a bi-level optimisation (Bard, 2013; Von Stackelberg, 2010):

$$\begin{aligned} \min_{\psi} \quad & \mathbb{E}_{\mathcal{D}_i \sim p(\mathcal{T})} \mathbb{E}_{(\mathbf{x}_{ij}^{(v)}, y_{ij}^{(v)}) \sim \mathcal{D}_i^{(v)}} \mathbb{E}_{q(\theta; \psi)} \left[ \mathcal{L}_{ij}^{(v)} + \mathcal{L}_i^{(t)} \right] + D_{\text{KL}} [q(\theta; \psi) \parallel p(\theta)] \\ \text{s.t.} \quad & \lambda_i = \arg \min_{\lambda_i} \mathcal{L}_i^{(t)}. \end{aligned} \quad (8)$$

Since we rely on gradient descent to minimise the objective function in the lower-level of (8), we can omit  $\mathcal{L}_i^{(t)}$  from the upper-level (i.e., the objective function), as follows:

$$\begin{aligned} \min_{\psi} \quad & \mathbb{E}_{q(\theta; \psi)} \mathbb{E}_{\mathcal{D}_i \sim p(\mathcal{T})} \left[ \mathcal{L}_i^{(v)} \right] + D_{\text{KL}} [q(\theta; \psi) \parallel p(\theta)] \\ \text{s.t.} \quad & \lambda_i = \arg \min_{\lambda_i} \mathcal{L}_i^{(t)}, \end{aligned} \quad (9)$$

where

$$\mathcal{L}_i^{(v)} = \mathbb{E}_{(\mathbf{x}_{ij}^{(v)}, y_{ij}^{(v)}) \sim \mathcal{D}_i^{(v)}} \left[ \mathcal{L}_{ij}^{(v)} \right]. \quad (10)$$

There are two major issues related to the optimisation in (9):

- (i) how to evaluate the generalisation errors corresponding to the first term of the upper-level in (9) for:
  - unseen queried example  $(x_{ij}^{(v)}, y_{ij}^{(v)}) \sim (\mathcal{D}_i^{(v)} \setminus \hat{\mathcal{D}}_i^{(v)})$ , and
  - an unseen task  $\mathcal{D}_{T+1} = \{\mathcal{D}_{T+1}^{(t)}, \mathcal{D}_{T+1}^{(v)}\} \sim p(\mathcal{T})$ ,
- (ii) how to model  $q(\mathbf{w}_i; \lambda_i)$  obtained in (6) expressively, so that it can approximate  $p(\mathbf{w}_i | \mathcal{D}_i^{(t)}, \theta)$  accurately.

We derive a novel upper-bound to address the problem (i) in Section 3.2, and present an implicit modelling approach to address the problem (ii) in Section 3.3.

### 3.2 PAC-BAYES GENERALISATION BOUND

The novel bound on the generalisation error for the first term in (9) is shown in Theorem 1. Please refer to the Supplementary Material A for the proof.

**Theorem 1.** *The general error of few-shot meta-learning (or, first term in (9)) can be approximately upper-bounded as:*

$$p \left( \mathbb{E}_{\theta \sim q(\theta; \psi)} \mathbb{E}_{\mathcal{D}_i \sim p(\mathcal{T})} \left[ \mathcal{L}_i^{(v)} \right] \leq \frac{1}{T} \sum_{i=1}^T \mathbb{E}_{\theta \sim q(\theta; \psi)} \left[ \hat{\mathcal{L}}_i^{(v)} + R_i \right] + R_0 \right) \geq 1 - \delta,$$

where  $\mathcal{L}_i^{(v)}$  is defined in Eq. 10,  $\delta \in (0, 1]$ , and:

$$\hat{\mathcal{L}}_i^{(v)} = \frac{1}{m_i^{(v)}} \sum_{j=1}^{m_i^{(v)}} \mathcal{L}_{ij}^{(v)} \quad (11)$$

$$R_0 = \sqrt{\frac{D_{\text{KL}} [q(\theta; \psi) \| p(\theta)] + \ln \frac{T(T+1)}{\delta}}{2(T-1)}} \quad (12)$$

$$R_i = \sqrt{\frac{D_{\text{KL}} [q(\mathbf{w}_i; \lambda_i) \| p(\mathbf{w}_i; \theta)] + \ln \frac{m_i^{(v)}(T+1)}{\delta}}{2(m_i^{(v)} - 1)}}. \quad (13)$$

The PAC-Bayes upper-bound in Theorem 1 upper-bounds the true error by three terms: (i) the empirical error on the available tasks and queried samples in the training set, (ii) the regularisation for the generalisation error due to unseen tasks  $R_0$ , and (iii) the regularisation for the generalisation error due to unseen queried samples  $R_i$ .

Given the PAC-Bayes bound in Theorem 1, our objective function in (9) can be written as:

$$\begin{aligned} \min_{\psi} \mathcal{L} &= \mathbb{E}_{q(\theta; \psi)} \left[ \frac{1}{T} \sum_{i=1}^T \hat{\mathcal{L}}_i^{(v)} + R_i \right] + R_0 + D_{\text{KL}} [q(\theta; \psi) \| p(\theta)] \\ \text{s.t. } \lambda_i &= \arg \min_{\lambda_i} \mathcal{L}_i^{(t)}. \end{aligned} \quad (14)$$

**Remark 1.** As shown in (14), our approach is a bi-level optimisation consisting of two steps. First, in the lower-level or task-adaptation step, we use VI with data likelihood evaluated on  $\mathcal{D}_i^{(t)}$  to correlate the prior  $p(\mathbf{w}_i; \theta)$  and the variational posterior  $q(\mathbf{w}_i; \lambda_i)$  of task-specific model parameter  $\mathbf{w}_i$  as shown in (6). Second, in the upper-level or meta-learning step, we optimise for the distribution  $q(\theta; \psi)$  of the meta-parameter  $\theta$  by cross-validating  $q(\mathbf{w}_i; \lambda_i)$  – learnt in the lower-level – on  $\mathcal{D}_i^{(v)}$ . The cost function of the upper-level optimisation consists of the PAC-Bayes bound in Theorem 1 and a regularisation term as shown in (14). In this procedure, the distribution  $q(\mathbf{w}_i; \lambda_i)$  of task-specific model parameters and its prior  $q(\theta; \psi)$  are learnt from  $\mathcal{D}_i^{(t)}$  and  $\mathcal{D}_i^{(v)}$ , respectively, and hence, satisfies the assumption of PAC-Bayes learning, which learns these distributions on separated data (Parrado-Hernández et al., 2012).

**Remark 2.** The results in Theorem 1 is different from MLAP (Amit & Meir, 2018), which is also meta-learning method derived based on PAC-Bayes bound, at the correlation between the prior  $p(\mathbf{w}_i; \theta)$  and the posterior  $q(\mathbf{w}_i; \lambda_i)$  of task-specific model parameter  $\mathbf{w}_i$ . MLAP (Amit & Meir, 2018) is formulated based on an upper-bound, where  $p(\mathbf{w}_i; \theta)$  and  $q(\mathbf{w}_i; \lambda_i)$  are correlated under a non-Bayesian setting. More specifically, they are learnt simultaneously through a single optimisation that minimises that upper-bound, resulting in a training procedure identical to the multi-task learning approach (Amit & Meir, 2018, Section 4.4). In contrast, we derive an upper-bound where the correlation between  $p(\mathbf{w}_i; \theta)$  and  $q(\mathbf{w}_i; \lambda_i)$  follows a Bayesian setting. We formulate the learning problem into a bi-level optimisation shown in (14), where in the lower-level, we explicitly correlate  $p(\mathbf{w}_i; \theta)$  and  $q(\mathbf{w}_i; \lambda_i)$  using variational Bayes inference with the data likelihood evaluated from the support set  $\mathcal{D}_i^{(t)}$ , and in the upper-level, we optimise for  $q(\theta; \psi)$  by cross-validating all  $q(\mathbf{w}_i; \lambda_i)$ , learnt in the lower-level on their corresponding query sets  $\mathcal{D}_i^{(v)}$ . This difference between the two methods is mostly due to their designated purposes: MLAP targets the multi-task learning setting with an extension to life-long learning, while our approach – similarly to MAML – is designed for few-shot learning setting (Amit & Meir, 2018, Section 5). Evidently, MLAP is tested only on a small number of tasks (less than 10), where each task has many training examples (about 2000) (Amit & Meir, 2018, Section 5), while our approach can be trained on millions of tasks, where each task has only a few examples (see Section 4). To further demonstrate this difference between the two approaches, we re-implement and modify MLAP based on their public code and run on the few-shot setting. As expected, MLAP performs as randomly as an arbitrary regression-er or classifier. We, therefore, exclude MLAP from all of our experiments presented in Section 4.

### 3.3 IMPLICIT VARIATIONAL DISTRIBUTION

In probabilistic statistics, the shared prior of model parameter,  $p(\mathbf{w}_i; \theta)$ , represents a modelling assumption, and the variational posterior of task-specific model parameter,  $q(\mathbf{w}_i; \lambda_i)$ , is a flexible function that can be adjusted to achieve a good trade-off between performance and complexity. In general,  $p(\mathbf{w}_i; \theta)$  and  $q(\mathbf{w}_i; \lambda_i)$  can be modelled using two general types of probabilistic models: prescribed and implicit (Diggle & Gratton, 1984). For example, ABML (Ravi & Beaton, 2019) is a prescribed approach where both distributions are assumed to be diagonal Gaussians. In this paper, we employ the implicit modelling approach to expressively represent  $p(\mathbf{w}_i; \theta)$  and  $q(\mathbf{w}_i; \lambda_i)$ .

Both distributions  $p(\mathbf{w}_i; \theta)$  and  $q(\mathbf{w}_i; \lambda_i)$  are now defined at a more fundamental level whereby data is generated through a stochastic mechanism without specifying parametric distributions. We use a parameterised model (i.e., a generator  $G$  represented by a deep neural network) to model the sample generation:

$$\begin{cases} \mathbf{w}_i \sim p(\mathbf{w}_i; \theta) & \Leftrightarrow \mathbf{w}_i = G(\mathbf{z}; \theta), \mathbf{z} \sim p(\mathbf{z}|\beta_i) \\ \mathbf{w}_i \sim q(\mathbf{w}_i; \lambda_i) & \Leftrightarrow \mathbf{w}_i = G(\mathbf{z}; \lambda_i), \mathbf{z} \sim p(\mathbf{z}|\beta_i), \end{cases} \quad (15)$$

where  $\mathbf{z} \in \mathbb{R}^Z$  is the latent noise,  $\beta_i$  is the parameter of the latent noise distribution  $p(\mathbf{z}|\beta_i)$ , which is learnt from the unlabelled data  $\mathbf{x}_{i,1:m_i^{(t)}}^{(t)}$  of the support set  $\mathcal{D}_i^{(t)}$ . One of the challenges to model  $p(\mathbf{z}|\beta_i)$  is the permutation invariance between training examples of the corresponding task  $\mathcal{T}_i$ . We, therefore, propose to use a pooling encoder to aggregate the output of unlabelled data:

$$\beta_i = \frac{1}{m_i^{(t)}} \sum_{k=1}^{m_i^{(t)}} \text{FC}_{\text{enc}}(\mathbf{x}_{ik}^{(t)}; \phi_{\text{enc}}), \quad (16)$$

where  $\text{FC}_{\text{enc}}(\cdot; \phi_{\text{enc}})$  represents an encoder parameterised by  $\phi_{\text{enc}}$ . In general,  $p(\mathbf{z}|\beta_i)$  can be any standard distribution that can be easily sampled from, such as a diagonal Gaussian. However, in the implementation, we observe that as the training task varies, the means and covariances of the Gaussian distribution (or  $\beta_i$ ) may vary drastically, resulting in a large variation of the latent noise sample  $\mathbf{z}$ , and potentially, making the training more difficult. To overcome that, we model  $p(\mathbf{z}|\beta_i)$  as a Beta distribution, where the sampling procedure produces a latent noise  $\mathbf{z} \in [0, 1]^Z$ . This constrains the latent noise space, resulting in a more stable training.

Due to the nature of implicit models, the KL divergence term of  $\mathcal{L}_i^{(t)}$  in (4), or in particular, the density ratio  $q(\mathbf{w}_i; \lambda_i)/p(\mathbf{w}_i; \theta)$ , cannot be evaluated either analytically or symbolically. We, therefore, propose to employ the *probabilistic classification* approach (Sugiyama et al., 2012, Chapter 4) to estimate the KL divergence term. We use a discriminator  $D$ , represented by a deep neural network with parameter  $\omega_i$ , as a classifier to distinguish different  $\mathbf{w}_i$  sampled from  $p(\mathbf{w}_i; \theta)$  (label 1) or  $q(\mathbf{w}_i; \lambda_i)$  (label 0). The objective function to train the discriminator  $D$  is:

$$\max_{\omega_i} \mathcal{L}_{\text{disc}}(\omega_i) = \mathbb{E}_{p(\mathbf{z})} [\ln D(G(\mathbf{z}; \theta); \omega_i)] + \mathbb{E}_{p(\mathbf{z})} [\ln (1 - D(G(\mathbf{z}; \lambda_i); \omega_i))]. \quad (17)$$

The KL divergence term of  $\mathcal{L}_i^{(t)}$  in (4) can, therefore, be estimated as <sup>2</sup>:

$$D_{\text{KL}} [q(\mathbf{w}_i; \lambda_i) \| p(\mathbf{w}_i; \theta)] \approx -\frac{1}{L_t} \sum_{l=1}^{L_t} V(G(\mathbf{z}^{(l)}; \lambda_i); \omega_i), \quad (18)$$

where  $\mathbf{z}^{(l)} \sim p(\mathbf{z}|\beta_i)$  defined in (15),  $L_t$  is the number of Monte Carlo samples, and  $V(\cdot, \omega_i)$  is the output of the discriminator  $D$  without sigmoid activation. In the implementation, we performing value clipping to ensure that the approximated KL divergence is non-negative.

The VFE in (6) can, therefore, be rewritten as:

$$\mathcal{L}_i^{(t)} \approx -\frac{1}{L_t} \sum_{l=1}^{L_t} \left[ V(G(\mathbf{z}^{(l)}; \lambda_i); \omega_i) + \sum_{k=1}^{m_i^{(t)}} \ln p(y_{ik}^{(t)} | \mathbf{x}_{ik}^{(t)}, G(\mathbf{z}^{(l)}; \lambda_i)) \right]. \quad (19)$$

<sup>2</sup>Refer to Supplementary Material B for details

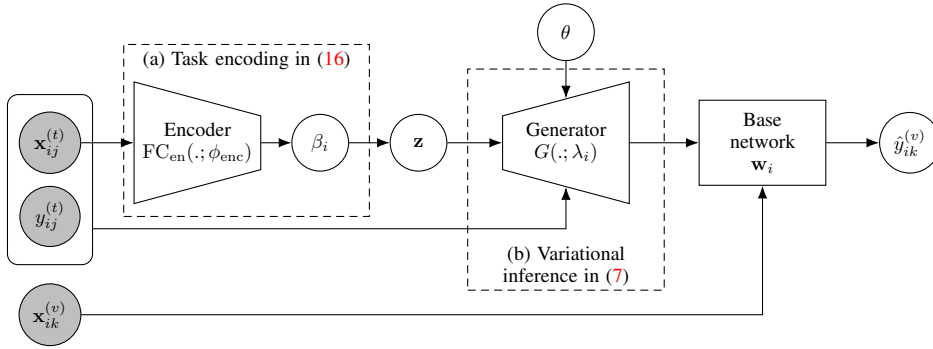


Figure 2: The proposed algorithm, SIMPa, consists of two phases illustrated in dashed rectangles: (a) task representation encoding, where unlabelled data is encoded using an encoder aggregator, and (b) gradient-based variational inference, where training data combined with the meta-parameter  $\theta$  is used to generate an adapted base network to solve the corresponding task.

One problem that arises when estimating the loss in (19) is how to obtain the local optimal parameters  $\omega_i^*$  for the discriminator  $D$ . One simple approach is to learn a different  $\omega_i$  for each different task  $\mathcal{T}_i$  by training the discriminator from scratch. The downside is the significant increase in training time and memory usage to store the computational graph to later be used for minimising the upper-bound in (14). To overcome this limitation, we propose to meta-learn  $\omega_i$  using MAML (Finn et al., 2017). In this scenario, we define  $\omega_0$  as the meta-parameters (or initialisation) of  $\omega_i$ . Within each task, we initialise  $\omega_i$  at  $\omega_0$  and use the generated  $w_i$  from (15) as training data. This approach leads to our proposed algorithm, named Statistical Implicit PAC-Bayes Meta-Learning (SIMPa), which can also be visualised in Figure 2. The details of the algorithm can be referred to Algorithms 1 and 2 in the Supplementary Material C for training and testing, respectively.

Another approach to estimate the KL divergence term of  $\mathcal{L}_i^{(t)}$  in (6) is to use a lower bound of f-divergence (Nguyen et al., 2010; Nowozin et al., 2016). There is a difference between the *lower bound of KL divergence approach* and the *probabilistic classification* presented in this subsection. In the former approach, the lower bound of the KL divergence is maximised to tighten the bound. In the latter approach, a discriminator is trained to minimise the logistic regression loss to estimate the ratio  $q(w_i; \lambda_i)/p(w_i; \theta)$ , and use Monte Carlo sampling to approximate the KL divergence of interest. Despite the difference mentioned above, the implementations of both approaches are quite similar. However, the *lower-bound of KL divergence* approach, with the computation of an exponential term in the objective function, suffers from numerical instability, especially at the beginning of training. As a result, we decide to use the *probabilistic classification* approach, where training process is numerically more stable.

One potential drawback of the implicit modelling approach is the curse of dimensionality, resulting in an expensive computation during training. This is an active research question when dealing with generative models in general. This issue can be addressed by encoding the high-dimensional data, such as images, to a feature embedding space by supervised-learning on the same training data set (Rusu et al., 2019). This strategy reduces the dimension of the input space, leading to smaller generator and discriminator models. The trade-off lies in the possibility of losing relevant information that can affect the performance on held-out tasks.

One advantage of our proposed method is the *task-awareness* due to the conditional latent noise distribution  $p(\mathbf{z}|\beta_i)$ . While other Bayesian few-shot meta-learning methods, such as PLATI-PUS (Finn et al., 2018) or ABML (Ravi & Beatson, 2019), randomly sample  $w_i$  from  $p(w_i; \theta)$ , our proposed SIMPa uses unlabelled data  $\mathbf{x}_{i,1:m_i}^{(t)} \sim \mathcal{D}_i^{(t)}$  to extract more information about the task  $\mathcal{T}_i$  when generating  $w_i$  as shown in (15), potentially resulting in a better adaptation.

It is also worth noting that our proposed method is easier to train than prior Bayesian few-shot meta-learning methods (Finn et al., 2018; Ravi & Beatson, 2019) because we no longer need to tune the weighting factor of the KL divergence term of  $\mathcal{L}_i^{(t)}$  in (6). Although weighting the KL divergence term can be justified by replacing the objective function in (6) by a constrained optimisation as shown in Beta-VAE (Higgins et al., 2016), the weighting factor is the corresponding Lagrange multiplier of

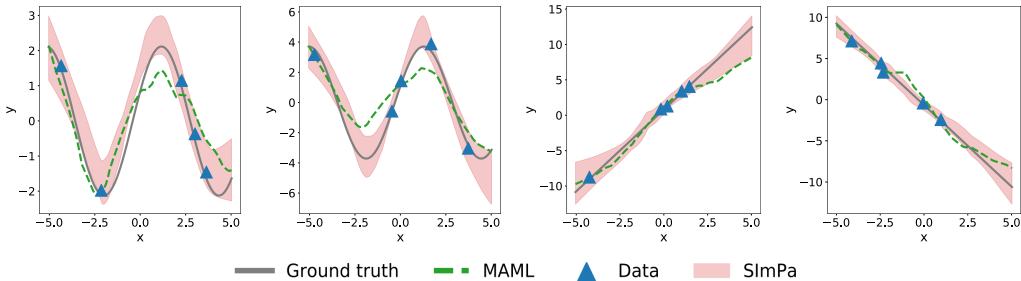


Figure 3: SImPa and MAML are compared in a regression problem when training is based on multi-modal data – half of the tasks are generated from sinusoidal functions, and the other half are from linear functions. The shaded area is the prediction made by SImPa  $\pm 3 \times$  standard deviation.

the constrained optimisation. Thus, simply setting that weighting factor as a tunable hyper-parameter may result in a sub-optimal solution for  $q(\mathbf{w}_i; \lambda_i)$ . In contrast, our proposed approach follows the standard variational approximation as shown in (6) without weighting the KL divergence term. The trade-off of our approach lies in the need to set the significance level  $\delta$ , but tuning  $\delta$  is arguably more intuitive than tuning the correct weighting factor for the KL divergence term.

## 4 EXPERIMENTAL EVALUATION

We evaluate SImPa on few-shot regression and classification problems. The loss functions used are mean-squared error and cross-entropy, respectively. Following the assumption of bounded losses made in Section 3.2, the losses in the derived upper-bound in Theorem 1 are clipped to  $[0, 1]$ . In addition, for simplicity, we limit our search to a family of diagonal Gaussian:  $q(\theta; \psi) = \mathcal{N}(\boldsymbol{\mu}_\theta, \sigma_\theta^2 \mathbf{I})$ , where  $\sigma_\theta$  is a hyper-parameter. This means  $\psi = \boldsymbol{\mu}_\theta$ . The meta-parameter  $\theta$  can, therefore, be sampled from  $q(\theta; \psi)$  by applying re-parameterisation trick. The prior  $p(\theta)$  is also assumed to be a diagonal Gaussian  $\mathcal{N}(\mu_0 \mathbf{1}, \sigma_0^2 \mathbf{I})$ . The KL divergence in (14) is, therefore, equivalent to a L2-regularisation for  $\boldsymbol{\mu}_\theta$ .

### 4.1 REGRESSION

The experiment in this subsection is a multi-modal task distribution where half of the data is generated from sinusoidal functions, while the other half is from linear functions (Finn et al., 2018). The sinusoidal function used in this experiment is in the form  $y = A \sin(x + \Phi) + \varepsilon$ , where  $A$  and  $\Phi$  are uniformly sampled from  $[0.1, 5]$  and  $[0, \pi]$ , respectively, while the linear function considered is in the form  $y = ax + b + \varepsilon$ , where  $a$  and  $b$  are randomly sampled from  $[-5, 5]$ . The noise  $\varepsilon$  is sampled from  $\mathcal{N}(0, 0.3^2)$ . The experiment is carried out under the 5-shot setting ( $m_i^{(t)} = 5$ ), and the validation set  $\hat{\mathcal{D}}_i^{(v)}$  consists of  $m_i^{(v)} = 15$  data points. The details of the experimental setup and additional visualisation results are presented in Supplementary Material D.

As shown in Figure 3, SImPa is able to vary the prediction variance, especially when there is more uncertainty in the training data, while MAML can only output a single value at each data point. For a quantitative comparison, we train many probabilistic meta-learning methods, including PLATIPUS (Finn et al., 2018), BMAML (Yoon et al., 2018) and ABML (Ravi & Beatson, 2019), in the same regression problem. Here, BMAML consists of 10 particles trained without Chaser Loss, and ABML is trained with a uniform hyper-posterior. As shown in Figure 4a, SImPa achieves much smaller negative log-likelihood (NLL), comparing to MAML, PLATIPUS and ABML, and comparable NLL to the non-parametric BMAML. To further evaluate the predictive uncertainty, we employ the reliability diagram based on the quantile calibration for regression (Song et al., 2019). The reliability diagram shows a correlation between predicted and actual probability. A perfectly calibrated model will have its predicted probability equal to the actual probability, and hence, align well with the diagonal  $y = x$ . The results in Figure 4b show that the model trained with SImPa achieves the best calibration among all the methods considered. Due to the nature of a deterministic approach, MAML (Finn et al., 2017) is represented as a horizontal line, resulting in a poor calibrated model.



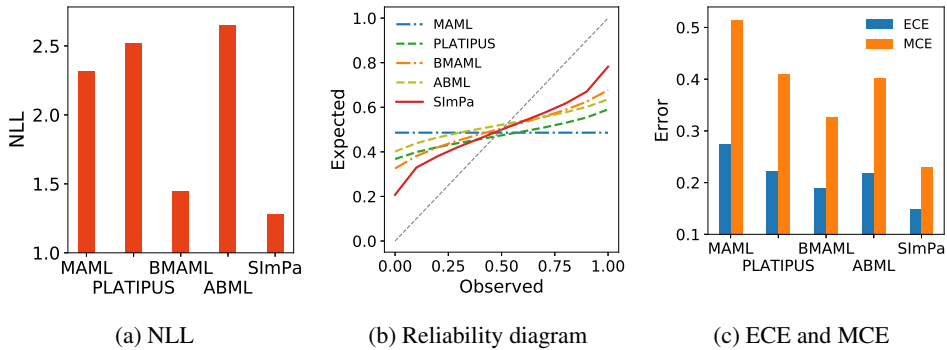


Figure 4: Quantitative comparison between various probabilistic meta-learning approaches averaged over 1000 unseen tasks shows that SImPa has the smallest NLL and calibration errors.

The two probabilistic meta-learning methods, PLATIPUS and ABML, perform better than MAML; however, the averaged slopes of their performance curves are quite close to MAML, implying that their diagonal Gaussian posteriors of task-specific model parameters have small covariances. This may be caused by their exclusive reliance on less-expressive diagonal Gaussian variational distributions. The performance of BMAML is slightly better than PLATIPUS and ABML due to its non-parametric modelling approach. In contrast, SImPa employs a much richer variational distribution for task specific parameters, and therefore, produces a model with better calibration. For another quantitative comparison, we plot the expected calibration error (ECE) (Guo et al., 2017), which is the weighted average of the absolute errors measuring from the diagonal, and the maximum calibration error (MCE) (Guo et al., 2017), which returns the maximum of absolute errors in Figure 4c. Overall, SImPa outperforms all of the state-of-the-art methods in both ECE and MCE.

#### 4.2 FEW-SHOT CLASSIFICATION

We evaluate SImPa on the  $N$ -way  $k$ -shot setting, where a meta learner is trained on many related tasks containing  $N$  classes with  $k$  examples per class ( $m_i^{(t)} = kN$ ). The evaluation is carried out by comparing the results of SImPa against the results of state-of-the-art methods on two few-shot learning benchmarking data sets: mini-ImageNet (Vinyals et al., 2016; Ravi & Larochelle, 2017) and tiered-ImageNet (Ren et al., 2018).

Mini-ImageNet has 100 classes with each class containing 600 colour images taken from ImageNet (Russakovsky et al., 2015). This data set represents a common benchmark for few-shot learning (Vinyals et al., 2016). We follow the standard train-test split which uses 64 classes for training, 16 classes for validation, and 20 classes for testing (Ravi & Larochelle, 2017). The images in the data set are pre-processed by down-sampling to 84-by-84 pixels before any training is carried out.

Tiered-ImageNet is one of the largest subsets of ImageNet, which consists of total 608 classes grouped into 34 high-level categories (Ren et al., 2018). Tiered-ImageNet is often used as a benchmark for large-scaled few-shot learning. We also follow the standard train-test split that consists of 20 categories for training, 6 categories for validation, and 8 categories for testing. In addition, our evaluation is carried out by employing the features extracted from a residual network trained on the data and classes from the training set (Rusu et al., 2019).

Two architectures of the base network have been employed in the experiment: “standard” 4-layer convolutional module network (Vinyals et al., 2016; Ravi & Larochelle, 2017; Finn et al., 2017) when the raw image data is used, and a customised fully connected network when extracted features (Rusu et al., 2019) are used. Please refer to Supplementary Material E for further details of the network architectures used for the base network, encoder, generator and discriminator, as well as the hyper-parameters.

<sup>3</sup>Trained on 30-way 1-shot setting

<sup>4</sup>Use extracted features (Rusu et al., 2019) as input

METHOD	1-SHOT	5-SHOT
<b>Mini-ImageNet (Ravi &amp; Larochelle, 2017) - standard 4-block CNN</b>		
Matching nets (Vinyals et al., 2016)	43.56 ± 0.84	55.31 ± 0.73
Meta-learner LSTM (Ravi & Larochelle, 2017)	43.44 ± 0.77	60.60 ± 0.71
MAML (Finn et al., 2017)	48.70 ± 1.84	63.15 ± 0.91
Prototypical nets (Snell et al., 2017) <sup>3</sup>	49.42 ± 0.78	<b>68.20 ± 0.66</b>
LLAMA (Grant et al., 2018)	49.40 ± 1.83	-
PLATIPUS (Finn et al., 2018)	50.13 ± 1.86	-
ABML (Ravi & Beatson, 2019)	45.00 ± 0.60	-
<b>SImPa</b>	<b>52.11 ± 0.43</b>	63.87 ± 0.35
<b>Mini-ImageNet (Ravi &amp; Larochelle, 2017) - non-standard network</b>		
Relation nets (Sung et al., 2018)	50.44 ± 0.82	65.32 ± 0.70
VERSA (Gordon et al., 2019)	53.40 ± 1.82	67.37 ± 0.86
SNAIL (Mishra et al., 2018)	55.71 ± 0.99	68.88 ± 0.92
adaResNet (Munkhdalai et al., 2018)	56.88 ± 0.62	71.94 ± 0.57
TADAM (Oreshkin et al., 2018)	58.50 ± 0.30	76.70 ± 0.30
LEO (Rusu et al., 2019)	61.76 ± 0.08	77.59 ± 0.12
LGM-Net (Li et al., 2019)	<b>69.13 ± 0.35</b>	71.18 ± 0.68
<b>SImPa<sup>4</sup></b>	63.73 ± 0.57	<b>78.04 ± 0.45</b>
<b>Tiered-ImageNet (Ren et al., 2018)</b>		
MAML (Liu et al., 2018)	51.67 ± 1.81	70.30 ± 0.08
Proto. Nets (Ren et al., 2018)	53.31 ± 0.89	72.69 ± 0.74
Relation Net (Liu et al., 2018)	54.48 ± 0.93	71.32 ± 0.78
Trns. Prp. Nets (Liu et al., 2018)	57.41 ± 0.94	71.55 ± 0.74
LEO (Rusu et al., 2019)	66.33 ± 0.05	81.44 ± 0.09
MetaOptNet (Lee et al., 2019)	65.81 ± 0.74	81.75 ± 0.53
<b>SImPa<sup>4</sup></b>	<b>70.82 ± 0.33</b>	<b>81.84 ± 0.21</b>

Table 1: The few-shot 5-way classification accuracy results (in percentage, with 95% confidence interval) of SImPa averaged over 600 tasks in comparison with state-of-the-art methods on mini-ImageNet (top and middle) and tiered-ImageNet (bottom) datasets. Overall, SImPa is competitive, and outperforms the state-of-the-art in some settings.

We report the classification accuracy of SImPa on these two data sets in Table 1. For mini-ImageNet, SImPa achieves the best results for the 1-shot setting when the base model is the “standard” CNN, and for the 5-shot setting when a different network architecture is used. SImPa shows the second best results for the 5-shot setting with the 4-layer CNN and the 1-shot setting with the different network architecture. Note that for the 5-shot setting using standard CNN, Prototypical networks need to train with a much higher “way” setting. For tiered-ImageNet, SImPa outperforms the current state-of-the-art on both 1- and 5-shot settings. To obtain a fairer comparison, we re-run MAML on the image data of mini-ImageNet using a ResNet10, which has about 5 million parameters (ours has about 8 millions parameters). However, MAML, with and without L2 regularisation, over-fits to training data (our best result was 89% accuracy on train, while only 42% on test). This known issue of overfitting when using larger networks in MAML was mentioned in the MAML’s paper (Finn et al., 2017, Section 5.2). We even try the similar model for ABML (Ravi & Beatson, 2019), but observed no improvement.

Similarly to the experiment for regression, we use reliability diagrams (Guo et al., 2017) to evaluate the predictive uncertainty. For a fair comparison, we re-implement several probabilistic meta-learning approaches, including MAML (Finn et al., 2017), PLATIPUS (Finn et al., 2018), BMAML (Yoon et al., 2018) and ABML (Ravi & Beatson, 2019), using the base model of a 4-block CNN, train under the same setting, and plot their reliability chart. The performance curves in the reliability diagram show how well calibrated a model is when testing across many unseen tasks. A perfectly calibrated model will have its values overlapped with the identity function  $y = x$ , indicating that the probability associated with the label prediction is the same as the true probability. To ease the visualisation, we normalise the reliability chart by subtracting the predicted accuracy by

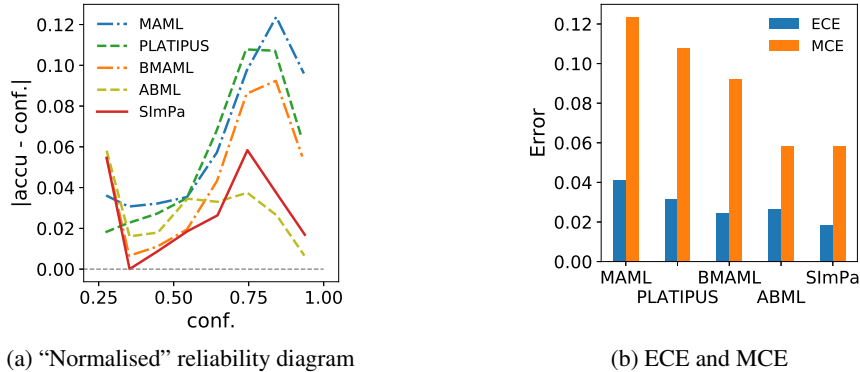


Figure 5: Calibration of the “standard” 4-block CNN trained with different meta-learning methods on 5-way 1-shot classification tasks on mini-ImageNet.

its corresponding value on the diagonal  $y = x$ , as shown in Figure 5a. Hence, for the normalised reliability chart, the closer to  $y = 0$ , the better the calibration. Visually, the model trained with SImPa shows better calibration than the ones trained with other meta-learning methods. To further evaluate, we compute the expected calibration error (ECE) and maximum calibration error (MCE) (Guo et al., 2017) of the models trained with these methods. The results plotted in Figure 5b show that the model trained with SImPa achieves the smallest ECE and MCE among all the methods considered in this comparison. The most competitive method to SImPa, regarding ECE and MCE, is ABML, but note that ABML has a much worse classification accuracy than SImPa, as shown in Table 1 (Top) – see row “ABML (Ravi & Beatson, 2019)”.

## 5 CONCLUSION

We introduce and formulate a new probabilistic algorithm for few-shot meta-learning. The proposed algorithm, SImPa, is based on PAC-Bayes framework which theoretically guarantees prediction generalisation on unseen tasks and samples. In addition, the proposed method employs a generative approach that implicitly models the prior of task-specific model parameter,  $p(\mathbf{w}_i; \theta)$ , shared across all tasks, and the task-specific posterior  $q(\mathbf{w}_i; \lambda_i)$ , resulting in more expressive variational approximation compared to the usual diagonal Gaussian methods, such as PLATIPUS (Finn et al., 2018) or ABML (Ravi & Beatson, 2019). The uncertainty, in the form of the learnt implicit distributions, can introduce more variability into the decision made by the model, resulting in well-calibrated and highly-accurate prediction. The algorithm can be combined with different base models that are trainable with gradient-based optimisation, and is applicable in regression and classification. We demonstrate that the algorithm has state-of-the-art calibration and prediction results on unseen data in a multi-modal 5-shot learning regression problem, and achieve state-of-the-art calibration and classification results on few-shot 5-way tasks on mini-ImageNet and tiered-ImageNet data sets.

## REFERENCES

- Ron Amit and Ron Meir. Meta-learning by adjusting priors based on extended PAC-Bayes theory. In *International Conference on Machine Learning*, pp. 205–214, 2018.
- Jonathan F Bard. *Practical bilevel optimization: algorithms and applications*, volume 30. Springer Science & Business Media, 2013.
- Jonathan Baxter. A model of inductive bias learning. *Journal of Artificial Intelligence Research*, 12: 149–198, 2000.
- Shai Ben-David, John Blitzer, Koby Crammer, Alex Kulesza, Fernando Pereira, and Jennifer Wortman Vaughan. A theory of learning from different domains. *Machine learning*, 79(1-2):151–175, 2010.

- John S Bridle and Stephen J Cox. Recnorm: Simultaneous normalisation and classification applied to speech recognition. In *Advances in Neural Information Processing Systems*, pp. 234–240, 1991.
- Rich Caruana. Multitask learning. *Machine learning*, 28(1):41–75, 1997.
- Peter J Diggle and Richard J Gratton. Monte Carlo methods of inference for implicit statistical models. *Journal of the Royal Statistical Society: Series B (Methodological)*, 46(2):193–212, 1984.
- Chelsea Finn, Pieter Abbeel, and Sergey Levine. Model-agnostic meta-learning for fast adaptation of deep networks. In *International Conference on Machine Learning*, pp. 1126–1135, 2017.
- Chelsea Finn, Kelvin Xu, and Sergey Levine. Probabilistic model-agnostic meta-learning. In *Conference on Neural Information Processing Systems*, pp. 9537–9548, 2018.
- Xavier Glorot and Yoshua Bengio. Understanding the difficulty of training deep feedforward neural networks. In *International Conference on Artificial Intelligence and Statistics*, pp. 249–256, 2010.
- Jonathan Gordon, John Bronskill, Matthias Bauer, Sebastian Nowozin, and Richard Turner. Meta-learning probabilistic inference for prediction. In *International Conference on Learning Representations*, 2019.
- Erin Grant, Chelsea Finn, Sergey Levine, Trevor Darrell, and Thomas Griffiths. Recasting gradient-based meta-learning as hierarchical bayes. In *International Conference on Learning Representations*, 2018.
- Chuan Guo, Geoff Pleiss, Yu Sun, and Kilian Q. Weinberger. On calibration of modern neural networks. In *International Conference on Machine Learning*, 2017.
- Irina Higgins, Loic Matthey, Arka Pal, Christopher Burgess, Xavier Glorot, Matthew Botvinick, Shakir Mohamed, and Alexander Lerchner. Beta-VAE: Learning basic visual concepts with a constrained variational framework. In *International Conference on Learning Representation*, 2016.
- Diederik P Kingma and Jimmy Ba. Adam: A method for stochastic optimization. In *International Conference on Learning Representations*, 2015.
- Brenden M Lake, Ruslan Salakhutdinov, and Joshua B Tenenbaum. Human-level concept learning through probabilistic program induction. *Science*, 350(6266):1332–1338, 2015.
- Kwonjoon Lee, Subhransu Maji, Avinash Ravichandran, and Stefano Soatto. Meta-learning with differentiable convex optimization. In *Proceedings of the IEEE Conference on Computer Vision and Pattern Recognition*, pp. 10657–10665, 2019.
- Huaiyu Li, Weiming Dong, Xing Mei, Chongyang Ma, Feiyue Huang, and Bao-Gang Hu. LGM-Net: Learning to generate matching networks for few-shot learning. In *International Conference on Machine Learning*, pp. 3825–3834, 2019.
- Yanbin Liu, Juho Lee, Minseop Park, Saehoon Kim, Eunho Yang, Sung Ju Hwang, and Yi Yang. Transductive propagation network for few-shot learning. In *International Conference on Learning Representation*, 2018.
- David A McAllester. PAC-Bayesian model averaging. In *Annual Conference on Computational Learning Theory*, volume 99, pp. 164–170, 1999.
- Nikhil Mishra, Mostafa Rohaninejad, Xi Chen, and Pieter Abbeel. A simple neural attentive meta-learner. In *International Conference on Learning Representations*, 2018.
- Tsendsuren Munkhdalai and Hong Yu. Meta networks. In *International Conference on Machine Learning*, 2017.
- Tsendsuren Munkhdalai, Xingdi Yuan, Soroush Mehri, and Adam Trischler. Rapid adaptation with conditionally shifted neurons. In *International Conference on Machine Learning*, pp. 3661–3670, 2018.

- XuanLong Nguyen, Martin J Wainwright, and Michael I Jordan. Estimating divergence functionals and the likelihood ratio by convex risk minimization. *IEEE Transactions on Information Theory*, 56(11):5847–5861, 2010.
- Sebastian Nowozin, Botond Cseke, and Ryota Tomioka. F-GAN: Training generative neural samplers using variational divergence minimization. In *Advances in neural information processing systems*, pp. 271–279, 2016.
- Boris N Oreshkin, Alexandre Lacoste, and Pau Rodriguez. TADAM: Task dependent adaptive metric for improved few-shot learning. In *Conference on Neural Information Processing Systems*, pp. 719–729, 2018.
- Emilio Parrado-Hernández, Amiran Ambroladze, John Shawe-Taylor, and Shiliang Sun. PAC-Bayes bounds with data dependent priors. *Journal of Machine Learning Research*, 13(Dec):3507–3531, 2012.
- Anastasia Pentina and Christoph Lampert. A PAC-Bayesian bound for lifelong learning. In *International Conference on Machine Learning*, pp. 991–999, 2014.
- Sachin Ravi and Alex Beatson. Amortized bayesian meta-learning. In *International Conference on Learning Representations*, 2019.
- Sachin Ravi and Hugo Larochelle. Optimization as a model for few-shot learning. In *International Conference on Learning Representations*, 2017.
- Mengye Ren, Eleni Triantafillou, Sachin Ravi, Jake Snell, Kevin Swersky, Joshua B Tenenbaum, Hugo Larochelle, and Richard S Zemel. Meta-learning for semi-supervised few-shot classification. In *International Conference on Learning Representation*, 2018.
- Michael T Rosenstein, Zvika Marx, Leslie Pack Kaelbling, and Thomas G Dietterich. To transfer or not to transfer. In *NIPS 2005 workshop on transfer learning*, volume 898, pp. 1–4, 2005.
- Olga Russakovsky, Jia Deng, Hao Su, Jonathan Krause, Sanjeev Satheesh, Sean Ma, Zhiheng Huang, Andrej Karpathy, Aditya Khosla, Michael Bernstein, Alexander C. Berg, and Li Fei-Fei. ImageNet Large Scale Visual Recognition Challenge. *International Journal of Computer Vision (IJCV)*, 115(3):211–252, 2015.
- Andrei A Rusu, Dushyant Rao, Jakub Sygnowski, Oriol Vinyals, Razvan Pascanu, Simon Osindero, and Raia Hadsell. Meta-learning with latent embedding optimization. In *International Conference on Learning Representations*, 2019.
- Adam Santoro, Sergey Bartunov, Matthew Botvinick, Daan Wierstra, and Timothy Lillicrap. Meta-learning with memory-augmented neural networks. In *International Conference on Machine Learning*, pp. 1842–1850, 2016.
- Jürgen Schmidhuber. *Evolutionary principles in self-referential learning (On learning how to learn: the meta-meta-... hook)*. Diploma thesis, Technische Universität München, 1987.
- Jake Snell, Kevin Swersky, and Richard Zemel. Prototypical networks for few-shot learning. In *Advances in Neural Information Processing Systems*, pp. 4077–4087, 2017.
- Hao Song, Tom Diethe, Meelis Kull, and Peter Flach. Distribution calibration for regression. In *International Conference on Machine Learning*, pp. 5897–5906, 6 2019.
- Masashi Sugiyama, Taiji Suzuki, and Takafumi Kanamori. *Density ratio estimation in machine learning*. Cambridge University Press, 2012.
- Flood Sung, Yongxin Yang, Li Zhang, Tao Xiang, Philip H.S. Torr, and Timothy M. Hospedales. Learning to compare: Relation network for few-shot learning. In *Conference on Computer Vision and Pattern Recognition*, 2018.
- Sebastian Thrun and Lorien Pratt. *Learning to learn*. Springer Science & Business Media, 1998.
- Oriol Vinyals, Charles Blundell, Tim Lillicrap, Daan Wierstra, et al. Matching networks for one shot learning. In *Advances in Neural Information Processing Systems*, pp. 3630–3638, 2016.

Heinrich Von Stackelberg. *Market structure and equilibrium*. Springer Science & Business Media, 2010.

Jaesik Yoon, Taesup Kim, Ousmane Dia, Sungwoong Kim, Yoshua Bengio, and Sungjin Ahn. Bayesian model-agnostic meta-learning. In *Advances in Neural Information Processing Systems 31*, pp. 7343–7353, 2018.

Ruixiang Zhang, Tong Che, Zoubin Ghahramani, Yoshua Bengio, and Yangqiu Song. MetaGAN: An adversarial approach to few-shot learning. In *Advances in Neural Information Processing Systems 31*, pp. 2371–2380, 2018.

## A PROOF OF PAC-BAYES FEW-SHOT META-LEARNING BOUND

The derivation is divided into three steps. The first two steps are to derive the PAC-Bayes bound for the generalisation errors induced by the unseen tasks, and the unseen queried examples. The final step is to combine the results to obtain a final bound shown in Theorem 1.

To prove Theorem 1, we employ the general form of the PAC-Bayes bound for a single-task setting (McAllester, 1999) stated in Theorem 2.

**Theorem 2** ((McAllester, 1999)). *Let  $\mathcal{D}$  be an arbitrary distribution over an example domain  $\mathcal{Z}$ . Let  $\mathcal{H}$  be a hypothesis class,  $\ell : \mathcal{H} \times \mathcal{Z} \rightarrow [0, 1]$  be a loss function,  $\pi$  be a prior distribution over  $\mathcal{H}$ , and  $\delta \in (0, 1]$ . If  $\mathcal{S} = \{z_j\}_{j=1}^m$  is an i.i.d. training set sampled according to  $\mathcal{D}$ , then for any “posterior”  $Q$  over  $\mathcal{H}$ , the following holds:*

$$p \left( \mathbb{E}_{z_j \sim p(z)} \mathbb{E}_{q \sim Q} \ell(q, z_j) \leq \mathbb{E}_{z_j \sim \mathcal{S}} \mathbb{E}_{q \sim Q} \ell(q, z_j) + \sqrt{\frac{D_{\text{KL}}[Q \|\pi] + \log \frac{m}{\delta}}{2(m-1)}} \right) \geq 1 - \delta.$$

Theorem 2 indicates that with a high probability, the expected error of an arbitrary posterior  $Q$  on data distribution  $p(z)$  is upper-bounded by the empirical error plus a complexity regularisation term. These two terms express the trade-off between fitting data (bias) and regularising model complexity (variance).

### A.1 PAC-BAYES BOUND FOR UNSEEN TASKS

We use Theorem 2 with the following substitutions: the loss function is  $\mathcal{L}_i^{(v)}$  defined in Eq. (10), the i.i.d. sample is the task-specific dataset:  $\mathcal{D}_i = \mathcal{D}_i^{(t)} \cup \mathcal{D}_i^{(v)}$ , sampled from the task distribution  $p(\mathcal{T})$ , the hypothesis is the meta-parameter  $\theta$ , the prior of the hypothesis is  $p(\theta)$ , the posterior is the variational posterior  $q(\theta; \psi)$  of the meta-parameter  $\theta$  introduced in (1). This leads to Corollary 1.

**Corollary 1** (PAC-Bayes bound for unseen task).

$$p \left( \mathbb{E}_{\mathcal{D}_i \sim p(\mathcal{T})} \mathbb{E}_{\theta \sim q(\theta; \psi)} \left[ \mathcal{L}_i^{(v)} \right] \leq \frac{1}{T} \sum_{i=1}^T \mathbb{E}_{\theta \sim q(\theta; \psi)} \left[ \mathcal{L}_i^{(v)} \right] + \tilde{R}_0 \right) \geq 1 - \delta_0,$$

where  $\delta_0 \in (0, 1]$ , and:

$$\tilde{R}_0 = \sqrt{\frac{D_{\text{KL}}[q(\theta; \psi) \|\ p(\theta)] + \ln \frac{T}{\delta_0}}{2(T-1)}}.$$

### A.2 PAC-BAYES BOUND FOR QUERIED EXAMPLES OF A SINGLE-TASK

We also employ Theorem 2, where the loss is  $[-\ln p(y_{ij}^{(v)} | \mathbf{x}_{ij}^{(v)}, \mathbf{w}_i)]$ , the i.i.d. sample is  $(\mathbf{x}_{ij}^{(v)}, y_{ij}^{(v)})$ , the hypothesis is task-specific parameters  $\mathbf{w}_i$ , the prior of the hypothesis is  $p(\mathbf{w}_i; \theta)$ , the posterior of the hypothesis is  $q(\mathbf{w}_i; \lambda_i)$ . Note that:

$$\mathcal{L}_{ij}^{(v)} = \mathbb{E}_{q(\mathbf{w}_i; \lambda_i)} \left[ -\ln p(y_{ij}^{(v)} | \mathbf{x}_{ij}^{(v)}, \mathbf{w}_i) \right] \quad (3)$$

$$\mathcal{L}_i^{(v)} = \mathbb{E}_{(\mathbf{x}_{ij}^{(v)}, y_{ij}^{(v)}) \sim \mathcal{D}_i^{(v)}} \left[ \mathcal{L}_{ij}^{(v)} \right] \quad (10)$$

$$\hat{\mathcal{L}}_i^{(v)} = \frac{1}{m_i^{(v)}} \sum_{j=1}^{m_i^{(v)}} \mathcal{L}_{ij}^{(v)}. \quad (\text{Theorem 1})$$

This leads to Corollary 2.

**Corollary 2** (PAC-Bayes bound for unseen examples of a single-task). *For any  $\delta_i \in (0, 1]$ , the following holds:*

$$p \left( \mathbb{E}_{(\mathbf{x}_{ij}^{(v)}, y_{ij}^{(v)}) \sim \mathcal{D}_i^{(v)}} \mathbb{E}_{\mathbf{w}_i \sim q(\mathbf{w}_i; \lambda_i)} \left[ -\ln p(y_{ij}^{(v)} | \mathbf{x}_{ij}^{(v)}, \mathbf{w}_i) \right] \leq \frac{1}{m_i^{(v)}} \sum_{j=1}^{m_i^{(v)}} \mathbb{E}_{q(\mathbf{w}_i; \lambda_i)} \left[ -\ln p(y_{ij}^{(v)} | \mathbf{x}_{ij}^{(v)}, \mathbf{w}_i) \right] + \tilde{R}_i \right) \geq 1 - \delta_i$$

or :  $p \left( \mathcal{L}_i^{(v)} \leq \hat{\mathcal{L}}_i^{(v)} + \tilde{R}_i \right) \geq 1 - \delta_i,$

where:

$$\tilde{R}_i = \sqrt{\frac{D_{\text{KL}} [q(\mathbf{w}_i; \lambda_i) \| p(\mathbf{w}_i; \theta)] + \ln \frac{m_i^{(v)}}{\delta_i}}{2(m_i^{(v)} - 1)}}.$$

### A.3 PAC-BAYES BOUND FOR META-LEARNING

We combine the results in Corollaries 1 and 2 to derive a novel PAC-Bayes bound for the first term in (9). For convenience, we restate the PAC-Bayes bound of interest as below.

**Theorem 1.** *The general error of few-shot meta-learning (or, first term in (9)) can be approximately upper-bounded as:*

$$p \left( \mathbb{E}_{\theta \sim q(\theta; \psi)} \mathbb{E}_{\mathcal{D}_i \sim p(T)} \left[ \mathcal{L}_i^{(v)} \right] \leq \frac{1}{T} \sum_{i=1}^T \mathbb{E}_{\theta \sim q(\theta; \psi)} \left[ \hat{\mathcal{L}}_i^{(v)} + R_i \right] + R_0 \right) \geq 1 - \delta,$$

*Proof.* First, we extend the bound for the unseen examples of a single-task obtained in Corollary 2 to many tasks. We apply the inequality in Lemma 3 (presented in Supplementary Material F) for Corollary 2 with the following substitution:  $X_i = \mathcal{L}_i^{(v)}$ ,  $Y_i = \hat{\mathcal{L}}_i^{(v)} + \tilde{R}_i$ ,  $n = T$ ,  $\delta_i = \delta_i$  gives:

$$p \left( \sum_{i=1}^T \mathcal{L}_i^{(v)} \leq \sum_{i=1}^T \hat{\mathcal{L}}_i^{(v)} + \tilde{R}_i \right) \geq 1 - \sum_{i=1}^T \delta_i.$$

Dividing both terms inside the probability by  $T$  gives:

$$p \left( \frac{1}{T} \sum_{i=1}^T \mathcal{L}_i^{(v)} \leq \frac{1}{T} \sum_{i=1}^T \hat{\mathcal{L}}_i^{(v)} + \tilde{R}_i \right) \geq 1 - \sum_{i=1}^T \delta_i. \quad (20)$$

Next, we need to prove the following:

**Proposition 1.** *If  $\theta$  is in a compact (closed and bounded) interval, and  $q(\theta; \psi) > 0$  is a continuous function in that interval, then:*

$$p \left( \frac{1}{T} \sum_{i=1}^T \mathbb{E}_{\theta \sim q(\theta; \psi)} \left[ \mathcal{L}_i^{(v)} \right] \leq \frac{1}{T} \sum_{i=1}^T \mathbb{E}_{\theta \sim q(\theta; \psi)} \left[ \hat{\mathcal{L}}_i^{(v)} + \tilde{R}_i \right] \right) \geq 1 - \sum_{i=1}^T \delta_i.$$

*Proof.* Multiplying  $q(\theta; \psi) > 0$  into both terms inside the probability on the left-hand side of (20) gives:

$$p \left( \frac{1}{T} \sum_{i=1}^T q(\theta; \psi) \mathcal{L}_i^{(v)} \leq \frac{1}{T} \sum_{i=1}^T q(\theta; \psi) \left[ \hat{\mathcal{L}}_i^{(v)} + \tilde{R}_i \right] \right) \geq 1 - \sum_{i=1}^T \delta_i.$$

Since  $q(\theta; \psi)$ ,  $\mathcal{L}_i^{(v)}$ ,  $\hat{\mathcal{L}}_i^{(v)}$ , and  $\tilde{R}_i$  are continuous function w.r.t.  $\theta$ , and  $\theta$  is in a compact interval, both terms inside the probability on the left-hand side are Riemann integrable w.r.t.  $\theta$ . Hence, we can apply the monotone of Riemann integral that:

$$f(x) \geq g(x) \implies \int_a^b f(x) dx \geq \int_a^b g(x) dx$$



to obtain the following:

$$p \left( \frac{1}{T} \sum_{i=1}^T \int_{\theta} q(\theta; \psi) \mathcal{L}_i^{(v)} d\theta \leq \frac{1}{T} \sum_{i=1}^T \int_{\theta} q(\theta; \psi) [\hat{\mathcal{L}}_i^{(v)} + \tilde{R}_i] d\theta \right) \geq 1 - \sum_{i=1}^T \delta_i.$$

This completes the proof for Proposition 1.  $\square$

Given the results in Corollary 1 and Proposition 1, we can apply Corollary 3 in Supplementary Material F to obtain:

$$p \left( \mathbb{E}_{\mathcal{D}_i \sim p(\mathcal{T})} \mathbb{E}_{\theta \sim q(\theta; \psi)} [\mathcal{L}_i^{(v)}] \leq \frac{1}{T} \sum_{i=1}^T \mathbb{E}_{\theta \sim q(\theta; \psi)} [\hat{\mathcal{L}}_i^{(v)} + \tilde{R}_i] + \tilde{R}_0 \right) \geq 1 - \sum_{i=0}^T \delta_i. \quad (21)$$

Setting  $\delta_i = \delta/(T+1)$ ,  $i \in \{0, \dots, T\}$  completes the proof.  $\square$

## B DERIVATION OF KL DIVERGENCE IN (18)

$$D_{\text{KL}} [q(\mathbf{w}_i; \lambda_i) \| p(\mathbf{w}_i; \theta)] = \mathbb{E}_{q(\mathbf{w}_i; \lambda_i)} \left[ \ln \frac{q(\mathbf{w}_i; \lambda_i)}{p(\mathbf{w}_i; \theta)} \right] \approx \mathbb{E}_{q(\mathbf{w}_i; \lambda_i)} \left[ \ln \frac{1 - D(\mathbf{w}_i; \omega_i)}{D(\mathbf{w}_i; \omega_i)} \right].$$

Note that:

$$D(\mathbf{w}_i; \omega_i) = \text{sigmoid} [V(\mathbf{w}_i; \omega_i)],$$

and

$$\mathbf{w}_i \sim q(\mathbf{w}_i; \lambda_i) \Leftrightarrow \mathbf{w}_i = G(\mathbf{z}; \lambda_i). \quad (15)$$

The KL divergence can, therefore, be approximated as:

$$\begin{aligned} D_{\text{KL}} [q(\mathbf{w}_i; \lambda_i) \| p(\mathbf{w}_i; \theta)] &\approx \mathbb{E}_{q(\mathbf{w}_i; \lambda_i)} \left[ \ln \frac{1 - \text{sigmoid} [V(\mathbf{w}_i; \omega_i)]}{\text{sigmoid} [V(\mathbf{w}_i; \omega_i)]} \right] \\ &\approx -\mathbb{E}_{q(\mathbf{w}_i; \lambda_i)} [V(\mathbf{w}_i; \omega_i)] = -\mathbb{E}_{q(\mathbf{w}_i; \lambda_i)} [V(G(\mathbf{z}; \lambda_i); \omega_i)]. \end{aligned}$$

## C ALGORITHM OF SIMPA

**Algorithm 1** SimPa - train

---

**Input:** task distribution  $p(\mathcal{T})$  and hyper-parameters:  $T, L_t, L_v, L_D, \alpha_t, \alpha_v, \gamma_t, \gamma_v, \nu, \delta, \eta$   
**Output:** hyper-meta-parameters  $\psi$ , encoder parameters  $\phi_{\text{enc}}$  and discriminator meta-parameters  $\omega_0$

- 1: initialise  $\psi$ ,  $\phi_{\text{enc}}$  and  $\omega_0$
- 2: **while**  $\psi$  not converged **do**
- 3:   sample  $\theta^{(k)} \sim q(\theta; \psi), k \in \{1, \dots, K\}$
- 4:   sample tasks  $\mathcal{T}_i \sim p(\mathcal{T}), i \in \{1, \dots, T\}$
- 5:   **for** each  $\theta^{(k)}$  **do**
- 6:     **for** each task  $\mathcal{T}_i$  **do**
- 7:        $\lambda_i \leftarrow \theta^{(k)}$
- 8:        $\omega_i \leftarrow \omega_0$
- 9:        $\beta_i \leftarrow \frac{1}{m_i^{(t)}} \sum_{j=1}^{m_i^{(t)}} \text{FC}_{\text{enc}}(\mathbf{x}_{ij}; \phi_{\text{enc}})$  {Eq. 16}
- 10:       **repeat**
- 11:          sample  $\mathbf{z}_i^{(j)} \sim p(\mathbf{z}; \beta_i), j \in \{1, \dots, L_D\}$
- 12:           $\mathbf{w}_{(p),i}^{(j)} \leftarrow G(\mathbf{z}_i^{(j)}; \theta)$
- 13:           $\mathbf{w}_{(q),i}^{(j)} \leftarrow G(\mathbf{z}_i^{(j)}; \lambda_i)$
- 14:           $\omega_i \leftarrow \omega_i + \gamma_t \nabla_{\omega_i} \mathcal{L}_{\mathcal{D}_i}(\omega_i)$  {Eq. (17) - adapt discriminator}
- 15:          sample  $\mathbf{z}_i^{(l_t)} \sim p(\mathbf{z}; \beta_i), l_t \in \{1, \dots, L_t\}$
- 16:           $\hat{\mathbf{w}}_i^{(l_t)} \leftarrow G(\mathbf{z}_i^{(l_t)}; \lambda_i)$
- 17:           $\lambda_i \leftarrow \lambda_i - \alpha_t \nabla_{\lambda_i} \mathcal{L}_i^{(l_t)}$  {Eq. (19) - optimise lower-level, or task adaptation}
- 18:          **until**  $\eta$  times
- 19:          sample  $\mathbf{z}_i^{(l_v)} \sim p(\mathbf{z}; \beta_i), l_v \in \{1, \dots, L_v\}$
- 20:           $\hat{\mathbf{w}}_{(q),i}^{(l_v)} \leftarrow G(\mathbf{z}_i^{(l_v)}; \lambda_i)$
- 21:          calculate  $\hat{\mathcal{L}}_i^{(v)}(\theta)$  and  $R_i$  {Eqs. (11) and (13)}
- 22:          repeat steps 11 and 13 to calculate  $\mathcal{L}_{\mathcal{D}_i}(\omega_i)$  {Eq. 17}
- 23:       **end for**
- 24:     **end for**
- 25:      $\psi \leftarrow \psi - \frac{\alpha_v}{K} \sum_{k=1}^K \frac{\partial \theta^{(k)}}{\partial \psi} \nabla_{\theta} [\mathcal{L}]$  {Optimise upper-level}
- 26:      $\phi_{\text{enc}} \leftarrow \phi_{\text{enc}} - \frac{\nu}{T} \nabla_{\phi_{\text{enc}}} \sum_{i=1}^T [\hat{\mathcal{L}}_i^{(v)} + R_i]$
- 27:      $\omega_0 \leftarrow \omega_0 + \frac{\gamma_v}{T} \nabla_{\omega_0} \sum_{i=1}^T \mathcal{L}_{\mathcal{D}_i}(\omega_i)$
- 28: **end while**

---

**Algorithm 2** SImPa - test**Input:** unseen task  $\mathcal{T}_{T+1}$ , and parameters  $\psi$ ,  $\phi_{\text{enc}}$  and  $\omega_0$  obtained in the training phase**Output:** prediction  $y_{(T+1)j}^{(v)}$ 

- 1: sample  $\theta^{(k)} \sim q(\theta; \psi)$ ,  $k \in \{1, \dots, K\}$
- 2: **for** each  $\theta^{(k)}$  **do**
- 3:    $\lambda_i \leftarrow \theta^{(k)}$
- 4:    $\omega_i \leftarrow \omega_0$
- 5:    $\beta_i \leftarrow \frac{1}{m_i^{(t)}} \sum_{j=1}^{m_i^{(t)}} \text{FC}_{\text{enc}}(\mathbf{x}_{ij}; \phi_{\text{enc}})$  {Eq. 16}
- 6:   **repeat**
- 7:     sample  $\mathbf{z}_i^{(j)} \sim p(\mathbf{z}; \beta_i)$ ,  $j \in \{1, \dots, L_D\}$
- 8:      $\mathbf{w}_{(p),i}^{(j)} \leftarrow G(\mathbf{z}_i^{(j)}; \theta)$
- 9:      $\mathbf{w}_{(q),i}^{(j)} \leftarrow G(\mathbf{z}_i^{(j)}; \lambda_i)$
- 10:     $\omega_i \leftarrow \omega_i + \gamma_t \nabla_{\omega_i} \mathcal{L}_{\mathcal{D}_i}(\omega_i)$  {Eq. (17) - adapt discriminator}
- 11:    sample  $\mathbf{z}_i^{(l_t)} \sim p(\mathbf{z}; \beta_i)$ ,  $l_t \in \{1, \dots, L_t\}$
- 12:     $\hat{\mathbf{w}}_i^{(l_t)} \leftarrow G(\mathbf{z}_i^{(l_t)}; \lambda_i)$
- 13:    calculate  $\mathcal{L}_i^{(t)}(\lambda_i, \omega_i, \theta)$  {Eq. (19) - calculate VFE}
- 14:     $\lambda_i \leftarrow \lambda_i - \alpha_t \nabla_{\lambda_i} \mathcal{L}_i^{(t)}$  {Eq. (19) - optimise lower-level, or task adaptation}
- 15:    **until**  $\eta$  times
- 16:    sample  $\mathbf{z}_i^{(l_v)} \sim p(\mathbf{z}; \beta_i)$ ,  $l_v \in \{1, \dots, L_v\}$
- 17:     $\hat{\mathbf{w}}_i^{(l_v)} \leftarrow G(\mathbf{z}_i^{(l_v)}; \lambda_i)$
- 18:    calculate  $p_{l_v}^{(k)}(y_{T+1,j}^{(v)} | \mathbf{x}_{T+1,j}^{(v)}, \hat{\mathbf{w}}_i^{(l_v)})$
- 19:    average:  $p(y_{T+1,j}^{(v)} | \mathbf{x}_{T+1,j}^{(v)}, \mathcal{D}_{T+1}^{(t)}, \theta^{(k)}) = \frac{1}{L_v} \sum_{l_v=1}^{L_v} p(y_{T+1,j}^{(v)} | \mathbf{x}_{T+1,j}^{(v)}, \hat{\mathbf{w}}_i^{(l_v)})$
- 20: **end for**
- 21: final prediction:  $p(y_{T+1,j}^{(v)} | \mathbf{x}_{T+1,j}^{(v)}, \mathcal{D}_{T+1}^{(t)}, \psi) = \frac{1}{K} \sum_{k=1}^K p(y_{T+1,j}^{(v)} | \mathbf{x}_{T+1,j}^{(v)}, \mathcal{D}_{T+1}^{(t)}, \theta^{(k)})$

**D** SETUP OF REGRESSION EXPERIMENT

The base model used for SImPa in this regression experiment is a two-hidden-layer fully connected neural network, each having 40 nodes followed by ReLU activation. The dimension of the latent noise in (15) is  $Z = 40$ . The encoder  $\text{FC}_{\text{enc}}(\cdot; \phi_{\text{enc}})$  in (16) has the same architecture as the base network with the output layer having  $2 \times Z$  units since a Beta distribution has 2 parameters. The output of the encoder is then split into two halves, each assigned to  $\beta_{i1}$  and  $\beta_{i2}$ . The generator is a fully connected network with two hidden layers, containing 128 and 512 nodes, respectively. The discriminator is a three-hidden-layer fully connected network consisting of 512, 128, and 40 nodes, respectively. All the hidden layers of both the generator and discriminator are activated by ReLU, except that the output layers of the generator and discriminator are activated by tanh and sigmoid, respectively. The reason that tanh is used to activate the output of the generator is to limit the weights of the base network (similar to weight clipping) to prevent the not-a-number (NaN) error at the very beginning of training due to overflow. In addition, no batch normalisation is used across the base, encoder, generator and discriminator networks.

In the experiments, the significance level is  $\delta = 10^{-2}$ . The hyper-prior  $p(\theta)$  is assumed to  $\mathcal{N}(0, 100 \times \mathbf{I})$ . The numbers of Monte Carlo samples used to adapt to task and make prediction are  $L_t = L_v = 16$ . The number of samples of the base network weights used for adapting the discriminator is  $L_D = 128$ . The number of  $\theta$  sampled from  $q(\theta; \psi)$  is  $K = 4$ . The task-specific variational parameters  $\lambda_i$  and discriminator parameters  $\omega_i$  are estimated by performing 5 gradient updates with learning rates  $\alpha_t = 10^{-3}$  and  $\gamma_t = 10^{-4}$ , respectively. The hyper-meta-parameters of interest  $\psi$ , which are the prior of the generator's parameters, the parameters of the encoder  $\phi_{\text{enc}}$ , and the meta-parameters of the discriminator  $\omega_0$  are optimised by Adam optimisers (Kingma & Ba, 2015) with step sizes  $\alpha_v = 10^{-4}$  for the two former, and  $\gamma_v = 10^{-5}$  for the latter.

In addition, we provide more visualisations of regression results in Figure 6.

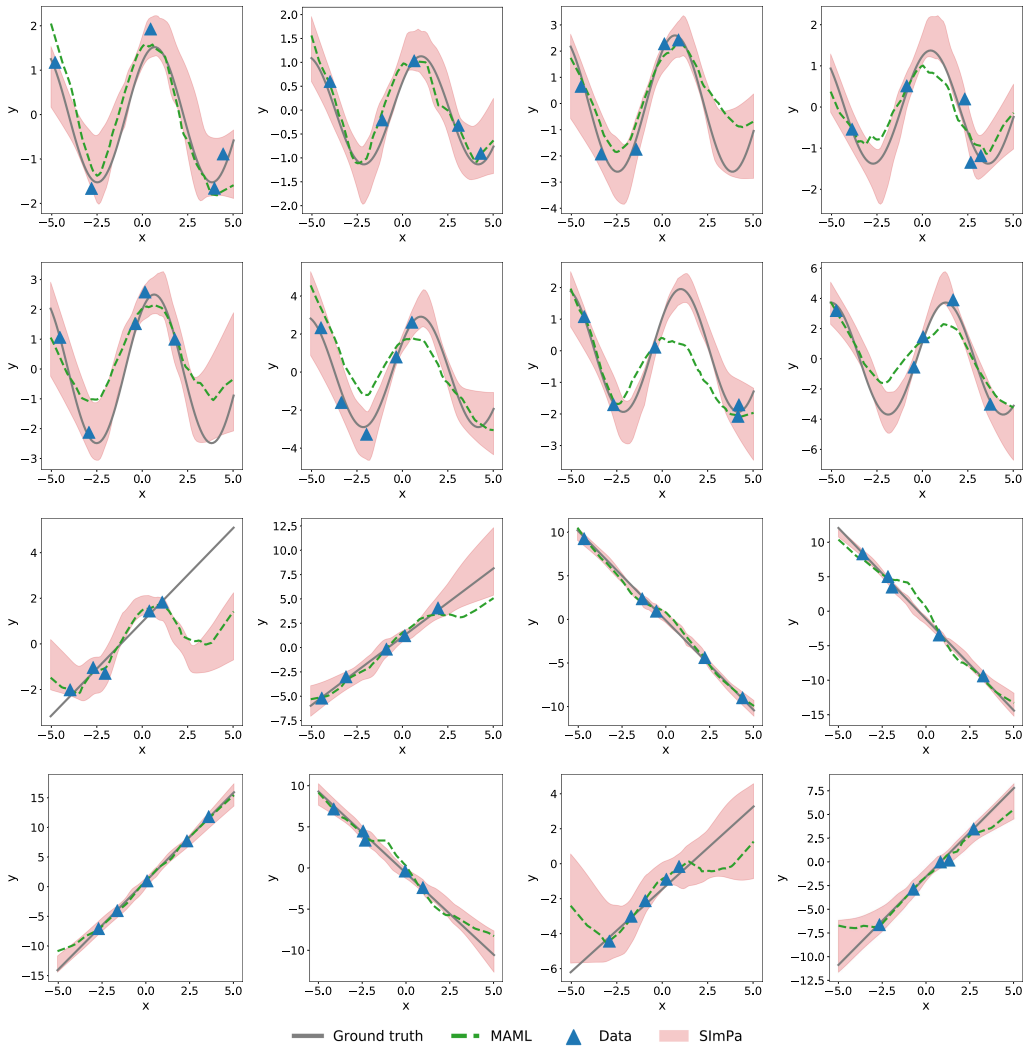


Figure 6: Additional visualisation for regression experiment with data generated from either a sinusoidal or linear function. The shaded area is the prediction made by SimPa with  $\pm 3$  standard deviation.

## E SETUP OF CLASSIFICATION EXPERIMENT

The setup of the  $N$ -way  $k$ -shot is done with the validation consisting of 15 examples in each class ( $m_i^{(t)} = kN$ , and  $m_i^{(v)} = 15N$ ). In addition, we apply label smoothing when training the discriminator by randomly sampling a real label from  $\mathcal{U}[0.95, 1]$ , and setting the fake label such that the sum of real and fake labels are 1. Without label smoothing, we observe that the discriminator over-fits very quickly at the beginning of training, resulting in learning a poor generator. This phenomena is well-known in GAN training. For the optimisation at task-level (or meta level), Adam optimiser is employed to optimise  $\psi$ ,  $\phi_{\text{enc}}$  and  $\omega_0$ . Please refer to Table 2 for detailed hyper-parameters used.

The dimension of the latent noise is  $Z = 128$ . The generator is a 2-layer fully-connected network with 256 and 512 hidden nodes. The discriminator is a 3-layer fully-connected network with 512, 256 and 128 hidden nodes. Different base- and encoder-networks are used in the experiments, depending on the input data.

During the training process, we observe that the generator often generates extremely large weights for the base network, resulting in an exploding gradient, and causing NAN errors. To constrain the value of the generated weights  $w_i$ , we apply the activation function  $\kappa \times \tanh(x/\kappa)$  on the output of

the generator (the effect is similar to clip in the range  $[-\kappa, \kappa]$ ). In the experiment for classification, we set  $\kappa = 20$ .

### E.1 STANDARD CNN WITH INPUT AS RAW IMAGE DATA

The base-network, in this case, is a standard 4-CNN-module network (Ravi & Larochelle, 2017; Finn et al., 2017). Each CNN-based module consists of a 3-by-3 convolution layer with 32 channels, followed by batch normalisation, ReLU and 2-by-2 max-pooling. This results in 800 nodes at the last convolutional module. These nodes are then fully connected to the output layer activated by softmax.

The encoder network shares a similar architecture, but has 5 modules, and the last module has 64 channels. Therefore, it output 128 features at the output. These output features are divided into half, and assigned to the 2 parameters of a Beta distribution which is used to model the latent noise.

### E.2 CUSTOMISED NETWORKS WITH INPUT AS EXTRACTED FEATURES

The base network is a fully-connected neural network with 2 hidden layers. These layers consist of 128 and 32 hidden nodes, respectively. ReLU is employed as the activation function without any batch normalisation.

The encoder is also a fully connected network with 2 hidden layers. Each layer consists of 256 hidden units activated by ReLU. No batch normalisation is employed. The output layer has 256 units, and divided into half and then assigned to the 2 parameters of a Beta distribution to model the latent noise.

Description	Notation	Standard CNN	Non-standard network
Confident level	$\delta$		0.1
Number of tasks per meta-update	$T$		2
Monte Carlo samples for $\theta$	$K$		2
Monte Carlo samples for $w_i$ at Eq. (7)	$L_t$	4	16
Monte Carlo samples for meta-update	$L_v$	4	16
Monte Carlo samples for discriminator	$L_d$		128
Learning rate for task-specific update	$\alpha_t$		$10^{-2}$
Learning rate for task-specific discriminator	$\gamma_t$		$10^{-4}$
Learning rate for meta-parameter	$\alpha_v$		$10^{-4}$
Learning rate for meta-discriminator	$\gamma_v$		$10^{-5}$
Learning rate for autoencoder	$\nu$		$10^{-4}$
Prior covariance of meta-parameter	$\sigma_\theta$		$10^{-8}$

Table 2: Hyper-parameters used in the classification experiments.

## F AUXILIARY LEMMAS

**Lemma 1.** For  $i = 1 : n$ , if  $X_i$  and  $Y_i$  are random variables, then:

$$p\left(\sum_{i=1}^n X_i \leq \sum_{i=1}^n Y_i\right) \geq p\left(\bigcap_{i=1}^n (X_i \leq Y_i)\right).$$

*Proof.* The proof is quite direct:

$$X_i \leq Y_i \implies \sum_{i=1}^n X_i \leq \sum_{i=1}^n Y_i. \tag{22}$$

Hence, the proof.  $\square$

**Lemma 2.** For  $n$  events  $A_i$  with  $i = 1 : n$ , the following holds:

$$p\left(\bigcap_{i=1}^n A_i\right) \geq \left(\sum_{i=1}^n p(A_i)\right) - (n-1), \forall n \geq 2.$$

*Proof.* Proof can be done by induction.

For  $n = 2$ :

$$p(A_1 \cap A_2) = p(A_1) + p(A_2) - p(A_1 \cup A_2) \geq p(A_1) + p(A_2) - 1.$$

Suppose that it is true for case  $n$ :

$$p\left(\bigcap_{i=1}^n A_i\right) \geq \left(\sum_{i=1}^n p(A_i)\right) - (n-1).$$

We prove that this is also true for case  $(n+1)$ :

$$\begin{aligned} p\left(\bigcap_{i=1}^{n+1} A_i\right) &= p\left(\bigcap_{i=1}^n A_i\right) + p(A_{n+1}) - p\left(\left(\bigcap_{i=1}^n A_i\right) \cup A_{n+1}\right) \\ &\geq p\left(\bigcap_{i=1}^n A_i\right) + p(A_{n+1}) - 1 \\ &\geq \left(\sum_{i=1}^n p(A_i)\right) - (n-1) + p(A_{n+1}) - 1 \\ &\quad \text{(assumption of induction for case } n\text{)} \\ &\geq \left(\sum_{i=1}^{n+1} p(A_i)\right) - ((n+1) - 1). \end{aligned}$$

It is, therefore, true for  $(n+1)$ , and hence, the proof.  $\square$

**Lemma 3.** Let  $X_i$  and  $Y_i$  are random variables with  $i = 1 : n$ . If  $p(X_i \leq Y_i) \geq 1 - \delta_i$  with  $\delta_i \in (0, 1]$ , then:

$$p\left(\sum_{i=1}^n X_i \leq \sum_{i=1}^n Y_i\right) \geq 1 - \sum_{i=1}^n \delta_i.$$

*Proof.* Applying Lemmas 1 and 2 for the left-hand side term of this lemma gives:

$$\begin{aligned} p\left(\sum_{i=1}^n X_i \leq \sum_{i=1}^n Y_i\right) &\geq p\left(\bigcap_{i=1}^n (X_i \leq Y_i)\right) \quad \text{(Lemma 1)} \\ &\geq \sum_{i=1}^n p((X_i \leq Y_i)) - (n-1) \quad \text{(Lemma 2)} \\ &\geq \sum_{i=1}^n (1 - \delta_i) - (n-1) \\ &= 1 - \sum_{i=1}^n \delta_i. \end{aligned} \tag{23}$$

$\square$

**Corollary 3.** If  $p(a \leq b) \geq 1 - \delta_1$  and  $p(b \leq c) \geq 1 - \delta_2$  with  $\delta_1, \delta_2 \in (0, 1]$ , then:

$$p(a \leq c) \geq 1 - \delta_1 - \delta_2.$$